Evaluation of safety of pointed masonry arches through the Static Theorem of Limit Analysis

E. De Rosa
University Federico II of Naples, Department of Costruzioni e Metodi Matematici in Architettura, Italy

F. Galizia
University Federico II of Naples, Department of Costruzioni e Metodi Matematici in Architettura, Italy

ABSTRACT: The analysis of mechanical behaviour of ancient masonry structures has been the subject of a rich literature until now. The results of lots of these works have underlined the particular importance of the Limit Analysis to estimate the safety of the masonries, when they are modeled as discrete systems of rigid blocks.

In the our study the safety of the masonry pointed arches has been pursued whether evaluating the collapse multiplier of the live loads, or calculating the lowest admissible thickness for assigned loads, by a linear formulation founded on the Static Theorem of the Limit Analysis.

The pointed masonry arches, discretized in rigid voussoirs, are studied with the assumption of inability to carry tension on the interfaces between the voussoir, of limited compressive strength and of sliding with dilatancy.

The solution and the evaluation of the collapse mechanism are obtained with Excel program's *solver*. Also the representation of this mechanism is pursued with *Excel.*

1 INTRODUTION

The aim of the our work has been to present a very simple numerical method, suitable to define the safety of the masonry made of stones even dry assembled or connected with joints filled by mortar, that are so typical of many ancient masonry cathedrals particularly in European countries. This objective has been achieved modelling the arch in rigid voussoirs and tacking account of a linear formulation founded on the Static Theorem of the Limit Analysis.
Its main mechanical features are:
- inability to carry tension for the contact interfaces;
- limited compressive strength at interfaces, obtained considering the closed parabolic N-M yield domain opportunely replaced by a piecewise linear yield domain having six or eight sides;
- provision for blocks to slide with dilatancy.

As far as it concerns the modeling -with regard to ordinary masonries made of stones, or of bricks having small dimensions compared with the dimensions of the structure-, we have verified that good results can be obtained already with a discretization of the masonry arches by a limited number rigid blocks. That involves a few number of unknowns and conditions and allows to obtain the solution very easily by the Excel program's *solver*.

When the static solution is obtained, the evaluation of the collapse mechanism is pursued with the respect of kinematic compatibility conditions.

2 THE PLANNING OF THE PROBLEM

2.1 The equilibrium conditions for the single voussoir

Because of symmetry, we refer to an generic half pointed arch discretized into *i* rigid voussoirs (*i* = 1 to *n*, being *n* the number of voussoirs). The generic voussoir is subjected to the stress resultants *N, T, M* -supposed to be applied in the centroid of each interface- and to the own weight P_i applied in its centre of gravity. Others loads can be eventually a fill $P_{i\,(R)}$, a wall $P_{i\,(M)}$, besides vertical or horizontal loads like distributed loads Q_i, or concentrated forces *F0, Fv, Fo* (Fig. 1). The equilibrium conditions for the generic voussoir are so formulated:

$$\mathbf{A^e X^e} + \mathbf{F_0^e} + \alpha\, \mathbf{F_1^e} = \mathbf{0} \tag{1}$$

where $\mathbf{A^e}$ is a matrix (3x6) depending on the voussoir's dimensions, $\mathbf{X^e}$ is the vector of the unknown stress resultants on the its two interfaces, $\mathbf{F_0^e}$ is the vector of the dead loads and $\mathbf{F_1^e}$ the vector of the live loads increasing by the multiplier α

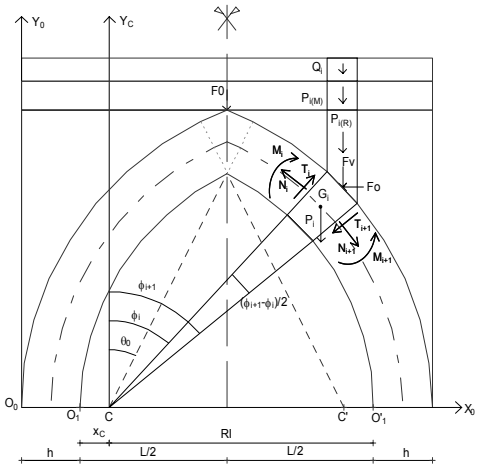

Figure 1 : Forces acting on the generic voussoir

2.2 Yield domain for the generic interface

The stress resultants on the interfaces have to respect the yield domains of the material for sliding and rocking. The yield domains of friction and that of rocking are showed in Figures. 2-3 where respectively φ_0 is the friction angle and $N°=\sigma°\cdot A$ is the limit compressive strength, being

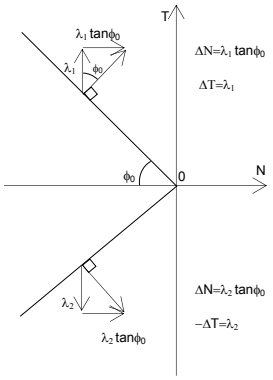

Figure 2 : Limit surface for sliding

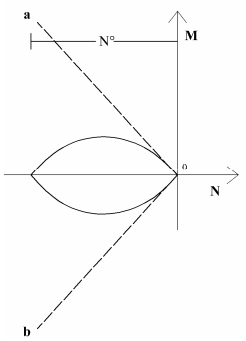

Figure 3 : Limit surface for rocking

σ° the limit compressive stress and $A=t\cdot h$ the cross-section area, where t is the thickness of arch and the depth h is the distance between the intrados and extrados lines.
The piecewise linearization of the yield domain in Figure 3 has been opportunely obtained by two polygons -one circumscribed and the other inscribed- having respectively six and eight sides (Figs.4-5).

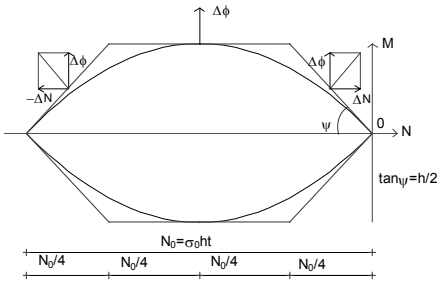

Figure 4 : Limit surface for rocking (circumscribed polygon).

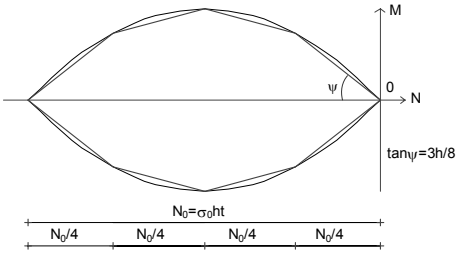

Figure 5 : Limit surface for rocking (inscribed polygon).

The conditions that have to be imposed on every generic interface, according to the kind of linearizated domain, respectively are:

$$\begin{bmatrix} tg\varphi_0 & 1 & 0 \\ tg\varphi_0 & -1 & 0 \\ h/2 & 0 & 1 \\ h/2 & 0 & -1 \\ 0 & 0 & 1 \\ 0 & 0 & -1 \\ -h/2 & 0 & 1 \\ -h/2 & 0 & -1 \end{bmatrix} \cdot \begin{bmatrix} N \\ T \\ M \end{bmatrix} - \begin{bmatrix} 0 \\ 0 \\ 0 \\ 0 \\ N°h/8 \\ N°h/8 \\ N°h/2 \\ N°h/2 \end{bmatrix} \leq \begin{bmatrix} 0 \\ 0 \\ 0 \\ 0 \\ 0 \\ 0 \\ 0 \\ 0 \end{bmatrix} \tag{2}$$

or:

$$\begin{bmatrix} tg\varphi_0 & 1 & 0 \\ tg\varphi_0 & -1 & 0 \\ 3h/8 & 0 & 1 \\ 3h/8 & 0 & -1 \\ h/8 & 0 & 1 \\ h/8 & 0 & -1 \\ -h/8 & 0 & 1 \\ -h/8 & 0 & -1 \\ -3h/8 & 0 & 1 \\ -3h/8 & 0 & -1 \end{bmatrix} \cdot \begin{bmatrix} N \\ T \\ M \end{bmatrix} - \begin{bmatrix} 0 \\ 0 \\ 0 \\ 0 \\ N°h/16 \\ N°h/16 \\ 3N°h/16 \\ 3N°h/16 \\ 3N°h/8 \\ 3N°h/8 \end{bmatrix} \leq \begin{bmatrix} 0 \\ 0 \\ 0 \\ 0 \\ 0 \\ 0 \\ 0 \\ 0 \\ 0 \\ 0 \end{bmatrix} \tag{3}$$

Obviously the domain (3) –inscribed polygon– is more restrictive of the domain (2)– circumscribed polygon– and gives advantage over safety.

2.3 Governing conditions

If *n* and *m* are respectively the number of the voussoirs and of interfaces, the equilibrium conditions are:

$$\mathbf{A}\,\mathbf{X} + \mathbf{F_0} + \alpha\,\mathbf{F_1} = \mathbf{0} \tag{4}$$

and the yield domain's conditions are:

$$\mathbf{Y} = \mathbf{DX} - \mathbf{TN} \leq \mathbf{0} \tag{5}$$

where **A** is a [3·*n* x 3·*m*] matrix, **X** is a 3·*m* vector, $\mathbf{F_0}$ and $\mathbf{F_1}$ are 3·*n* vectors, α is the unknown collapse multiplier, **D** is a (*k*·*m* x 3·*m*) matrix - where *k* is 8 or 10 according to yield domain (2) or (3) selected - and **TN** is a (k·*m*) vector of known terms.
The problem is resolved researching the maximum α subject to (4) and (5), with $\alpha \geq 0$.

We have obtained the solution of problem making use of *Excel*.

2.4 The evaluation of collapse mechanism

Once the multiplier α has been calculated we can pursue the kinematic problem having in account of the conditions:

$$\mathbf{A}^{\mathbf{T}}\mathbf{u} = \boldsymbol{\Delta} \tag{6}$$

and of the flow rule:

$$\boldsymbol{\Delta} = \mathbf{D}^{\mathbf{T}}\boldsymbol{\lambda} \tag{7}$$

being **u** the vector of the degrees of freedom (three for every voussoir), $\boldsymbol{\Delta}$ the vector which collects the displacements between the interfaces (three for every interface) and $\boldsymbol{\lambda}$ the vector of the generalized strain rates associated to the yield conditions (*k* for every interface).

We have pursued also this solution and its collapse configuration making use of *Excel.*

3 APPLICATIONS

3.1 Introduction

We have examined various types of pointed masonry arches, defined by the x-coordinate x_c of centroid C of the semi-arch regards to the point O_1 (Fig. 1) and by the length RI of the radius of intrados line. These two quantity are tied by the following relationships: $x_c = k_o L$; $RI = L(1 - k_o)$, being respectively k_o (k_o = 1/3, 1/4,…1/10,..) the coefficient that describes the generic type of pointed arch and L the generic span.
All the arches have been studied like a system of eighteen rigid voussoirs. We have used the inscribed yield domain (4) and the symmetry has been taken into account. For all the examples examined, have been assigned the following same data:

- span L = 4,5m
- thickness t = 1m
- limit compressive stress σ° = 4 MPa
- arch density γ_A = 16 KN/m^3
- fill density γ_f = 16 KN/m^3
- wall density γ_w = 16 KN/m^3
- wall height h_w = 1 m

3.2 Evaluation maximum loads multiplier

We have evaluated the collapse multiplier of various types of pointed masonry arches (h = 0.5 m) subjected to different loads (see table 1). Of some of them, the collapse configuration and moreover the curve of the pressures, the diagrams of compressive strength, of shear and of bending moment has been represented.

Table 1

			LOADS				Angle of internal friction	Multiplier of live loads
			Live Loads (KN)		Dead Loads (KN/m^3)			
Pointed Arches γ_A=16 KN/m^3; L= 4,5 m ; h =0,5 m			**F0**	**Q**	**Fill**	**Wall** (h_w=1m)	ϕ_0 (grades)	α
equilateral pointed arch			10				≥ 47	3,10
x_C (m)	θ_0	RI (m)	10		γ_f=16		≥ 57	9,18
0	0,5236	4,5		10			≥ 17	39,14
				10	γ_f=16		≥ 17	38,39
			10	10	γ_f=16	γ_w=16	≥ 24	21,05
1/10 pointed arch			10				≥ 42	2,73
x_C (m)	θ_0	RI (m)	10		γ_f=16		≥ 52	7,95
0,45	0,4605	4,05		10			≥ 18	38,07
				10	γ_f=16		≥ 18	37,77
			10	10	γ_f=16	γ_w=16	≥ 24	19,76
1/9 pointed arch			10				≥ 41	2,69
x_C (m)	θ_0	RI (m)	10		γ_f=16		≥ 51	7,81
0,5	0,4528	4		10			≥ 18	37,93
				10	γ_f=16		≥ 18	37,70
			10	10	γ_f=16	γ_w=16	≥ 22	19,60
1/8 pointed arch			10				≥ 40	2,63
x_C (m)	θ_0	RI (m)	10		γ_f=16		≥ 50	7,63
0,5625	0,4429	3,9375		10			≥ 18	37,74
				10	γ_f=16		≥ 18	37,60
			10	10	γ_f=16	γ_w=16	≥ 22	19,39
1/7 pointed arch			10				≥ 39	2,56
x_C (m)	θ_0	RI (m)	10		γ_f=16		≥ 49	7,40
0,642857	0,4297	3,8571		10			≥ 19	37,45
				10	γ_f=16		≥ 19	37,32
			10	10	γ_f=16	γ_w=16	≥ 22	19,10
1/6 pointed arch			10				≥ 38	2,47
x_C (m)	θ_0	RI (m)	10		γ_f=16		≥ 48	7,10
0,75	0,4115	3,75		10			≥ 19	37,13
				10	γ_f=16		≥ 19	36,98
			10	10	γ_f=16	γ_w=16	≥ 22	18,69
1/5 pointed arch			10				≥ 37	2,33
x_C (m)	θ_0	RI (m)	10		γ_f=16		≥ 47	6,65
0,9	0,3844	3,6		10			≥ 19	36,59
				10	γ_f=16		≥ 19	36,46
			10	10	γ_f=16	γ_w=16	≥ 22	18,12
1/4 pointed arch			10				≥ 35	2,12
x_C (m)	θ_0	RI (m)	10		γ_f=16		≥ 45	5,07
1,125	0,3398	3,375		10			≥ 20	35,70
				10	γ_f=16		≥ 20	35,58
			10	10	γ_f=16	γ_w=16	≥ 22	17,17
1/3 pointed arch			10				≥ 28	1,73
x_C (m)	θ_0	RI (m)	10		γ_f=16		≥ 38	4,80
1,5	0,2526	3		10			≥ 22	32,71
				10	γ_f=16		≥ 22	33,59
			10	10	γ_f=16	γ_w=16	≥ 25	15,43

Example 1: *Equilateral pointed arch subject to a live force F0=10KN acting on the axis of symmetry.*

For values of the friction angle $\varphi_0 \geq 47°$ the load's multiplier α results 3,10 and the collapse mechanism is characterized by five rocking crises (Fig. 6). In figure 7 is showed the curve of the pressures and in the Figures 8-10 are showed the compressive strength, the shear and the bending respectively.

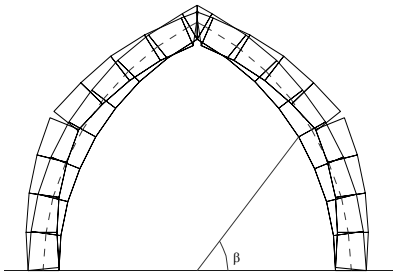

Figure 6 : Collapse mechanism

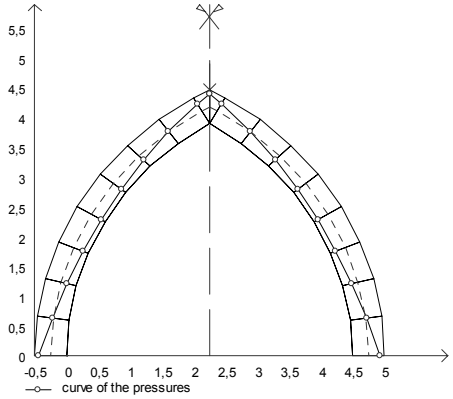

Figure 7 : Curve of the pressures

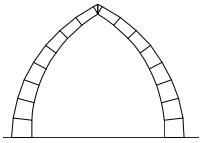

Figure 8 : Compressive strength

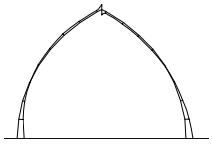

Figure 9 : Shear

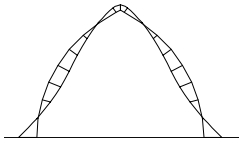

Figure 10 : Bending moment

Example 2: *Equilateral pointed arch subject to a live load distributed with a greater intensity on the abutments of arch ($Q_0 \div Q_4$=1KN; $Q_5 \div Q_8$=60KN).*

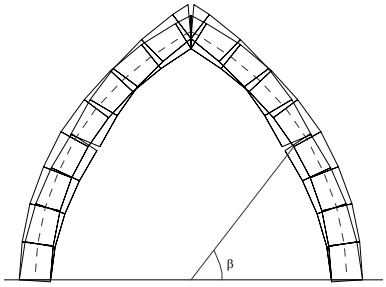

Figure 11 : Collapse mechanism

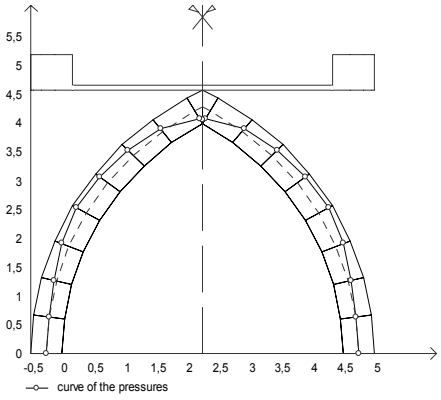

Figure 12 : Curve of the pressures

For values of the friction angle $\varphi_0 \geq 22°$ the load's multiplier α results 43,35 and its collapse mechanism (see Figure 11) is characterized as for the example previously examined still by five

rocking crises, but this time with opposite openings.

In Figures 12 is showed the curve of the pressures and in the Figures 13-15 are showed the compressive strength, the shear and the bending moment diagrams respectively. Besides we have found that in the two cases examined, increasing the quantity k_o, the multiplier α decreases always but the collapse mechanism never changes.

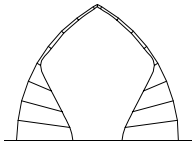

Figure 13 : Compressive strength

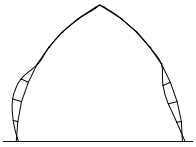

Figure 14 : Shear

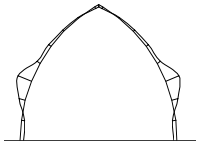

Figure 15 : Bending moment

Example 3: *Equilateral pointed arch subject to a force F0=10KN and an uniformly distributed load Q=10KN, as live loads and to the fill and to a wall (h_w=1m) up the fill, as dead loads.*

For values of the friction angle $\varphi_0 \geq 24°$ the load's multiplier α is 21,05 and the collapse mechanism is characterized by six rocking crises (Fig. 16). In Figure 17 is showed the curve of the pressures and in the Figures 18-20 are showed the compressive strength, the shear and the bending moment diagrams respectively.

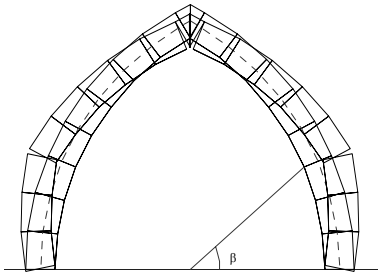

Figure 16 : Collapse mechanism

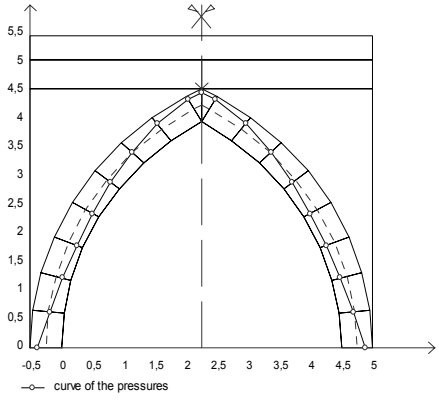

Figure 17 : Curve of the pressures

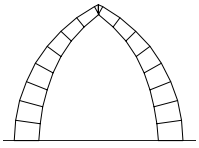

Figure 18 : Compressive strength

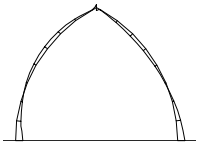

Figure 19 : Shear

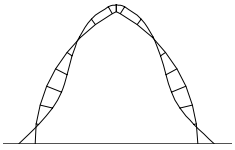

Figure 20 : Bending moment

Also in this case, varying the types of pointed arches, the multiplier α decreases (see table 1), but the collapse mechanism do not change excepted for the 1/3 pointed arch for that the collapse mechanism is characterized by five rocking crises (Fig. 21).

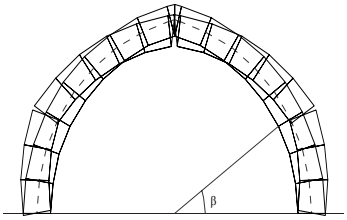

Figure 21 : 1/3 Pointed arch
collapse mechanism

3.3 Evaluation minimum depth h

A second application regards the evaluation of minimum depth h of various types of pointed masonry arches subjected to different loads (see table 2). Of some of them, the collapse configuration and moreover the curve of the pressures, the diagrams of compressive strength, of shear and of bending moment has been represented.

Example 4: *Equilateral pointed arch subject to a forceF0 =10 kN and a uniformly distributed load Q = 10 kN/m and to the fill and to a wall of height* h_w *= 1 m.*

For values of the friction angle $\varphi_0 \geq 17°$ the minimum depth h results 0,26 m and the collapse mechanism is characterized by six rocking crises (Fig. 22). In Figure 23 is showed the curve of the pressures and in the Figures 24-26 are showed the compressive strength, the shear and the bending moment diagrams respectively. Varying the types of pointed arches, the minimum depth h increases (see table 2).

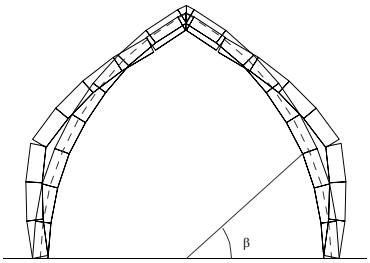

Figure 22 : Collapse mechanism

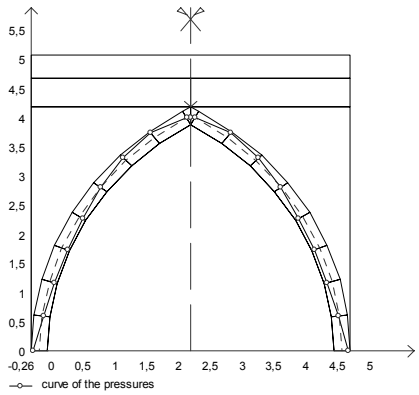

Figure 23 : Curve of the pressures

4. CONCLUSIONS

By the dates reported in the two tables it is possible to observe as, for the same loads and density of the materials, the highest load's multipliers and the lowest depts *h* are attained for the equilateral pointed arch. These results confirm that the stability and the safety of an arch grows greatly when the arches verge on a pointed shape and the arch that has a better behaviour is the equilateral pointed arch.
We have besides noted that for all the various types of pointed arches:
- the behavior essentially don't change varying the span L and the depth h, but change only the values of the multiplier.

- to obtain only rocking crises, the friction angle φ_0 doesn't can be smaller than a determinate value because in these cases there are sliding crises and the load's multiplier reduces.
- nothing changes increasing the minimum value of the friction angle required to obtain only rocking crises.

We have also verified as either the load's multipliers or the values of the friction angle required to obtain only rocking crises change taking into account the circumscribed yield domain (3).
For instance, for Example 3 the average increases of load's multipliers and of values of the friction angle are respectively of $5 \div 6\%$ and of $1 \div 2$ grades.

Table 2

			LOADS				Angle of internal friction	
Pointed Arches γ_A=16 KN/m^3; L= 4,5 m			**F0** (KN)	**Q** (KN)	**Fill** (KN/m^3)	**Wall** (KN/m^3) (h_w=1m)	ϕ_0 (grades)	**h** min (m)
equilateral pointed arch			10				≥ 31	≥ 0,35
x_C (m)	θ_0	RI (m)	10		γ_f=16		≥ 33	≥ 0,18
0	0,5236	4,5		10			≥ 25	≥ 0,29
				10	γ_f=16		≥ 28	≥ 0,27
			10	10	γ_f=16	γ_f=16	≥ 17	≥ 0,26
1/10 pointed arch			10				≥ 29	≥ 0,36
x_C (m)	θ_0	RI (m)	10		γ_f=16		≥ 30	≥ 0,18
0,45	0,4605	4,05		10			≥ 25	≥ 0,30
				10	γ_f=16		≥ 25	≥ 0,24
			10	10	γ_f=16	γ_f=16	≥ 17	≥ 0,27
1/9 pointed arch			10				≥ 28	≥ 0,37
x_C (m)	θ_0	RI (m)	10		γ_f=16		≥ 26	≥ 0,18
0,5	0,4528	4		10			≥ 26	≥ 0,30
				10	γ_f=16		≥ 26	≥ 0,24
			10	10	γ_f=16	γ_f=16	≥ 17	≥ 0,27
1/8 pointed arch			10				≥ 28	≥ 0,37
x_C (m)	θ_0	RI (m)	10		γ_f=16		≥ 26	≥ 0,18
0,5625	0,4429	3,937 5		10			≥ 27	≥ 0,30
				10	γ_f=16		≥ 27	≥ 0,23
			10	10	γ_f=16	γ_f=16	≥ 17	≥ 0,27
1/7 pointed arch			10				≥ 27	≥ 0,37
x_C (m)	θ_0	RI (m)	10		γ_f=16		≥ 26	≥ 0,19
0,64285 7	0,4297	3,857 1		10			≥ 24	≥ 0,30
				10	γ_f=16		≥ 24	≥ 0,23
			10	10	γ_f=16	γ_f=16	≥ 17	≥ 0,27
1/6 pointed arch			10				≥ 27	≥ 0,38
x_C (m)	θ_0	RI (m)	10		γ_f=16		≥ 26	≥ 0,19
0,75	0,4115	3,75		10			≥ 22	≥ 0,31
				10	γ_f=16		≥ 22	≥ 0,22
			10	10	γ_f=16	γ_f=16	≥ 17	≥ 0,28
1/5 pointed arch			10				≥ 26	≥ 0,38
x_C (m)	θ_0	RI (m)	10		γ_f=16		≥ 26	≥ 0,20
0,9	0,3844	3,6		10			≥ 19	≥ 0,31
				10	γ_f=16		≥ 21	≥ 0,21
			10	10	γ_f=16	γ_f=16	≥ 18	≥ 0,28
1/4 pointed arch			10				≥ 25	≥ 0,40
x_C (m)	θ_0	RI (m)	10		γ_f=16		≥ 26	≥ 0,21
1,125	0,3398	3,375		10			≥ 20	≥ 0.32
				10	γ_f=16		≥ 22	≥ 0,21
			10	10	γ_f=16	γ_f=16	≥ 18	≥ 0,29
1/3 pointed arch			10				≥ 24	≥ 0,43
x_C (m)	θ_0	RI (m)	10		γ_f=16		≥ 25	≥ 0,24
1,5	0,2526	3		10			≥ 24	≥ 0,33
				10	γ_f=16		≥ 24	≥ 0,23
			10	10	γ_f=16	γ_f=16	≥ 20	≥ 0,31

Taking into account the circumscribed yield domain equally we have noted a reduction of the values of minimum depth h. For instance, for Example 3 the average reduction is more than 30%.
In the end we have simulate the effect of a chain throw two horizontal forces Fo applied, once on the third last voussoirs and once on the last voussoirs, and we have checked a remarkable increase of load's multiplier, particularly when the forces are applied on the third last voussoirs. For instance for Example 3, for Fo = 250 KN, the load's multiplier increases more than 40% when the forces are on last voussoirs and more than 100% when the forces are on the third last voussoirs.

REFERENCES

Anselmi, C.A., De Rosa, E., Fino, L., 2004. Limit Analysis of Masonry Structures. *IV Simposio di Structural Analysis of Historical Constructions*, Padova, Italy, 1, 545-550.

Anselmi, C.A., De Rosa, E., Fino, L., 2005. Evaluation of collapse load for masonry walls, *10th Canadian Masonry Symposium*, Banff, Alberta.

Anselmi, C.A., De Rosa, E., Fino, L., 2006. Evaluation of static collapse multiplier for masonry walls subjected to out-of-plane loading. *7th International Masonry Conference*, Londra.

Franciosi, V., 1984. L'attrito nel calcolo a rottura delle murature. *Giornale del Genio Civile*, p. 215-234.

Gilbert, M., Melbourne, C., 1994. *Rigid-block Analysis of Masonry Structures*, The Structural Engineer,

Heyman, J., 1966. The Stone Skeleton. *International Journal Solids Structures*, p. 2, 249-279.

Heyman, J., 1968. The Safety of Masonry Arches, *International Journal Mechanical Sciences*, p.11, 363-38572, 21, 356-361.